FOCUS ON FUTURE TRENDS IN EXPERIMENTAL DETERMINATION OF CRACK INITIATION IN REINFORCED RUBBER

RADEK STOČEK[a,b], ONDŘEJ KRATINA[c], and IVO KUŘITKA[a]

[a] *Centre of Polymer Systems, University Institute, Tomas Bata University in Zlín, Nad Ovčírnou 3685, 760 01 Zlín,* [b] *PRL Polymer Research Lab., Nad Ovčírnou 3685, 760 01 Zlín,* [c] *Department of Polymer Engineering, Faculty of Technology, Tomas Bata University in Zlín*
stocek@cps.utb.cz

Keywords: crack propagation, fatigue analysis, fracture mechanics, vulcanized rubber

Abstract

We concentrate our work to the description of the state-of the-art and future trends in experimental laboratory characterization concerning structure-property relationship of unfilled and filler reinforced elastomers with respect to the micro-crack's initiation and its propagation under the behavior simulating the real loading conditions in practice. We theoretically describe the fracture mechanism leading to the micro-crack initiation and summarize the criterions, which are available for experimental characterization of rubber fracture. We describe how the micro-crack initiation could experimentally be analysed with common testing equipment. Finally we show how the experimental fracture analysis and surface investigation could contribute to a description of the interaction between micro-cracks initiation, fatigue and fracture crack propagation in rubber under the real dynamic loading conditions.

Introduction

The fracture of materials is mostly an undesirable process that reduces the service life of structural components. Defects on nano- as well as micro-scale commonly exist or arise due to exceeding of critical value of structure toughness in every real material and are the reason for creations of cracks on macro-scale. The fracture mechanics investigates the behaviour of an existent crack in a test specimen of a given material, whereas the theoretical background is given as well as for initiation of micro-crack but not supported with any experimental methodology in comparison to the macro-crack behavior. It is an important branch of material science and much effort has been already made to modify materials with the objective of preferably high fracture toughness at specified requirements with respect to other material properties.

Rubber materials are weakly cross-linked polymeric materials. Due to the high internal flexibility, rubbers exhibit large deformations even under weak external forces above the glass transition temperature. The rubber exhibit excellent damping behaviour and thereby the rubber has a broad using in industry and technique. Therefore the rubber is at most used in the application where high dynamically loading is applied on the rubber product. The most important high dynamically loaded technique rubber parts are e.g. tire, timing belt, pressure tube, rubber sealing, air shock absorber etc. Thus the dynamical loading the rubber are exposed to strong fatigue behavior leading to micro-crack initiation as well as its critical propagation. Thus the rubber materials are usually filled with hard nano-structured particles in order to enhance different mechanical properties such as strength, hardness, stiffness or abrasion resistance. The resulting multi-scale structural hierarchies due to the phase morphology, the distribution and dispersion of filler and the multi-scale structure of filler itself influences the fracture mechanical behaviour of rubber. Particularly these characteristic behaviours are based on the filler network build with the nanoparticles, size of filler cluster, interaction of filler-filler- and polymer-filler-bonds and the specific surface of filler under the identical compounding conditions[1,2]. Increased reinforcement of the rubber has been according to the fracture mechanics defined as increased crack growth or fatigue resistance[3].

Fracture mechanics of rubber on micro-scale

There are two known different effects in filled rubber, where the fracture of rubber matrix depends on the filler cluster breakdown. The breakdown process is termed as Mullins effect and is characterised due to stress-softening in rubber at large dynamic deformations[4]. Similar to large rubber test specimen deformations the breakdown process proceeds at small-strain dynamic deformations in dependence on dynamic viscoelastic properties of filled rubber and is termed as Payne-effect[1]. Raab at all showed in ref.[5] that the carbon-black or silica consist of particles with a rough surface forming aggregates in the 50–100 nm range and these lead to formation of filler agglomerates generally larger than 10 μm and are termed filler clusters. The filler cluster could be schematically substituted by circle of the same diameter as the largest dimension of cluster[6,7]. The cluster may be broken down into aggregates, but aggregates may not be broken down into primary particle[4]. Therefore the breakdown of cluster, respectively

the cluster dimension, hypothetically could define an initial length of the crack in rubber. Beside the mechanical energy could cause the rapture of more clusters at once and thus to initiate the crack over cluster length. To describe this phenomenon experimentally is a very important aim of high scientific interest, which will help to understand the fracture mechanics of rubber on the micro-scale.

For the carbon black filled elastomers differences between their resistance against crack initiation and propagation were found[1,2]. The reason for the decreasing of the crack resistance with higher filler content was found in the complexity of the filler network and ascribed to flash temperature effect within crack tip region[8,9]. Reincke described in ref.[9] that the material reinforced with silica showed a little different crack resistance behaviour compare to the rubber reinforced with carbon-black. This means, different mechanisms in carbon-black and silica-filled rubber must contribute to enhancement of crack resistance. It is known that due to their adjustable elastic and viscous properties, especially the fracture mechanics or crack growth depend on a lot of conditions and processing parameters, respectively. Thus to gain the physical understanding of crack initiation, propagation and tear resistance of elastomers or viscoelastic solids, there is a high scientific and technological potential for understanding of process influenced fundamental material specific fracture problems, specially due to the strongly non-linear deformation behaviour. The micromechanical mechanisms of crack initiation and propagation in elastomeric materials are subject of high scientific interest, because at present it is still not exactly known how these processes start and how they proceed under quasi-static as well as dynamic loading conditions. What are the reasons for the crack initiation, its propagation and what are the influences for the initiation time, crack growth velocity and crack growth orientation? These are the main important subjects of scientific research for investigating of fracture mechanics of elastomers. Most efforts in this field are based on the fundamental work of Rivlin and Thomas[10], whereas the fracture behaviours were investigated on the macro-scale and generalized an energy balance criterion for rubber.

Energy balance of rubber fracture

Due to the ability to large deformations, an elastic crack blunting can be observed, i.e. a crack opens up if the specimen is loaded. However, this crack tip blunting is reversible in contrast to the plastic crack blunting in metallic materials[12].

Generally the fracture theory is based on the crack propagation in the exact orthogonally direction to the main stress and describe the energy necessary for the creation of the new differential crack surface. It proposes, the strain energy release rate is the controlling parameter for crack growth and mathematically defined as,

$$T = -(\partial U / \partial A). \qquad (1)$$

Where, T is tearing energy, U is the elastic strain energy, A is the interfacial area of crack and partial derivative denotes that no external work is done on the system.

Energy balance can be evaluated from both, the experimental and the numerical side. Experimental characterization is related to the evaluation of energy taken from loading and unloading curves, whereas numerical evaluation can be either taken from loading and unloading curves or by determining of energy J-Integral[11]:

$$J_k = \int_R (W n_k + \sigma_{ji} n_j \frac{\partial u_i}{\partial x_k}) ds \qquad (2)$$

Where, W is the strain elastic energy density, n is the outer normal unit vector of R, σ is the stress tensor, u is the displacement vector and s is the element length.

The path independent of the J-integral allows an integration path, taken sufficiently far from the crack tip and thus the fracture parameters calculated with using J-integral are independent on the direction of the crack propagation[11]. The commonly using of the on- or off-line calculation of fracture parameters at the fatigue dynamic fracture tests are not state-of the-art, therefore the tearing energy criterion is commonly used for the fatigue dynamic fracture analysis.

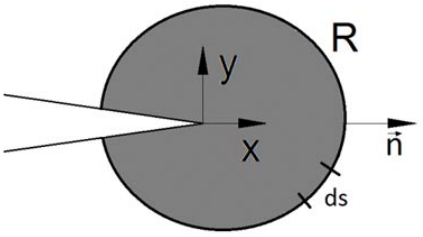

Fig. 1. **Definition of a contour R encircling the crack tip vicinity**

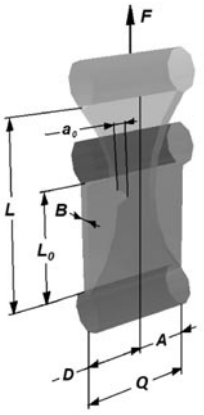

Fig. 2. **Schematic diagram of SENT test specimen**

Practice use of tearing energy

Rivlin & Thomas[10] formulated the tearing energy T for rubber in single edge notched tensile (SENT) as well as in pure-shear test specimens. For SENT test specimen (see. Fig. 2) with a notch on one side, the tearing energy is determined as follows:

$$T = 2 \cdot k \cdot w \cdot a \tag{3}$$

Where w is the strain elastic energy density stored in the un-notched test specimen, a – crack length and k – strain-dependent term. An approximate relation for k was determined by Lake[13]:

$$k = \frac{\alpha}{\sqrt{\lambda}} = \frac{\alpha}{\sqrt{1+\varepsilon}} \tag{4}$$

where λ = extension ratio; ε = strain and α is a fit parameter. Furthermore, it was found by Klüppel[8] that the parameter α does not agree with the literature value $\alpha = \pi = 3.14$ proposed by Gent[9]. The value of the parameter α has been determined by Klüppel[9] for various samples between 1.2 and 3.1. Thus the equation (*3*) takes than the following form:

$$T = \frac{2 \cdot \alpha}{\sqrt{\lambda}} \cdot w \cdot a = \frac{2 \cdot \alpha}{\sqrt{1+\varepsilon}} \cdot w \cdot a \tag{6}$$

Pure-shear test specimen is schematically visualized in the Fig. 3 and has been characterized with the notch length a_0, which develops into the crack length a and is sufficiently long compared to the length of test specimen L_0. The test specimen can be divided into different regions. Region A_1 is unstrained and region C-D is in pure-shear state, whereas the region C is identical with the pure-shear state region C in the un-notched test specimen visualized in the Figure 1 (right) and is geometrically defined as follows:

$$\lambda(x) = \frac{dx}{dx_0} = 1 \tag{7}$$

$$\lambda(y) = \frac{dy}{dy_0} = \frac{y}{y_0} = \varepsilon(y) + 1 \quad \Rightarrow \quad \begin{bmatrix} x \\ y \end{bmatrix} = \begin{bmatrix} 1 & 0 \\ 0 & \varepsilon(y)+1 \end{bmatrix} \cdot \begin{bmatrix} x_0 \\ y_0 \end{bmatrix}$$

Furthermore, there is an area of complicated strain around the crack tip in region D, and a region of edge effect shown as A, that is identical with edge effect region A of un-notched test specimen. The increasing of crack length by da, induces the moving of the region D along by da, but the pattern of strain, and hence the energy stored, remains unaltered. For a pure-shear test specimen's geometry the tearing energy T is considered to be independent of the crack length:

$$T = w \cdot L_0 \tag{8}$$

Where w is the strain elastic energy density stored in the un-notched test specimen and L_0 the length of not strained test specimen.

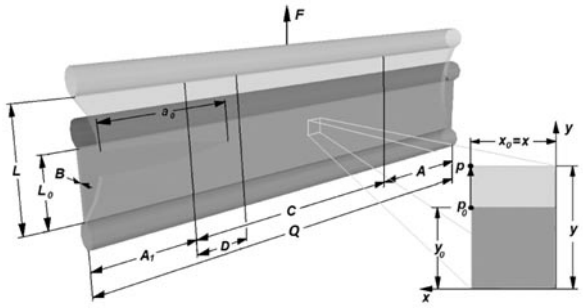

Fig. 3. **Schematic diagram of pure-shear test specimen with the visualisation of regions under different stress conditions**

Fracture mechanical treatment of failure due to fatigue loading

Gent, Lindley and Thomas[14] determined experimentally the crack growth rate *da/dn* in dependence on the tearing energy T for rubber materials. Figure 4 shows the typical relationship for a rubber material on a double logarithmic plot. Lake and Lindley[15] divided this plot into 4 regions which characterise different tear behaviours. The crack growth rate *da/dn* depends on the tearing energy T in each of the 4 regions in a characteristic manner.

As long as the value of tearing energy T is lower than T_0, crack growth proceeds at a constant rate r and the crack growth is independent of the dynamical loading, but

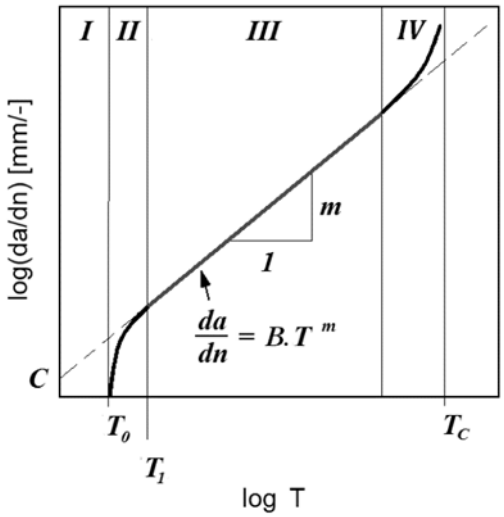

Fig. 4. **Double logarithmic plot of crack growth rate *da/dn vs.* tearing energy *T* for rubber material[15]**

affected by the environmental attack and the crack does not initiates.

$$T \le T_0 \Rightarrow \frac{da}{dn} = r \tag{9}$$

The criterion of crack initiation is situated to the boundary point between region I and II.

$$T = T_0 \Rightarrow \frac{da}{dn} = A(T - T_0) + r = r \tag{10}$$

In the region II between T_0 and T_1 one finds a transition between a nucleation and propagation of crack growth. The crack initiates in the range of the instable crack growth:

$$T_0 \le T \le T_I \Rightarrow \frac{da}{dn} = A(T - T_0) + r \tag{11}$$

After this transient state the crack propagates in a region between T_1 and T_C of stable crack growth which is denoted as region III. The relationship between fatigue crack growth rate *da/dn* and tearing energy describe Paris & Erdogan[16] with the power-law:

$$T_I \le T < T_C \Rightarrow \frac{da}{dn} = B \cdot \Delta T^m \tag{12}$$

where B and m are material constants. The region III was utilised as the region that corresponds most closely to crack growth rates found in the engineering fatigue range.

In the last region IV the tearing energy T_C proceeds to the instable state of crack growth and the crack growth rate will become essentially infinite.

$$T \approx T_C \Rightarrow \frac{da}{dn} = \infty \tag{13}$$

The relationship of crack initiation and crack growth was demonstrated in ref.[10,17] in the dependence of rubber type and thereby of chemical specification of uncured rubber components regarding to the experimental fatigue analysis of NR (natural rubber) and SBR (styrene-butadiene rubber). The results show, that in strain crystallising rubber such as NR the crack growth is delayed somehow by strain-induced crystallization at the crack tip. On the other hand, non-strain crystallising rubber like SBR will follow time-dependent crack growth behaviour. With the next increase of loading amplitude i.e. increase of tearing energy, the crack growth characteristics of both analysed elastomers show also a difference of crack growth increase as well. Gent et al.[14] observed by experimental comparison of NR and BR (Polybutadiene rubber), that the initiation of cracks in BR starts at higher tearing energy than in NR. Whereas the follows crack growth shows a counter phenomenon of more rapidly propagation of crack in BR in comparison to the rubber

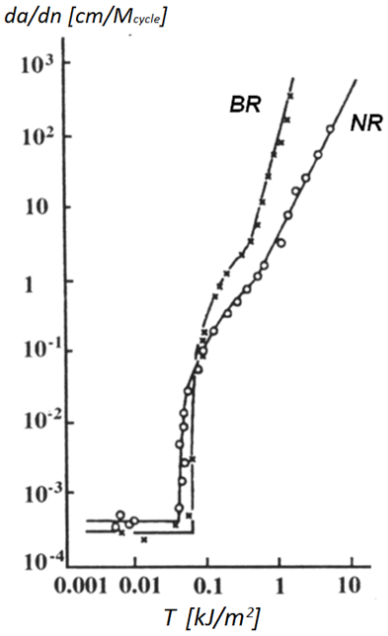

Fig. 5. **Relation between crack growth rate *da/dn* and tearing energy *T* of NR and BR[14]**

test specimen based on NR (s. Fig. 5). Could than the strain-induces anisotropy or nature matrix resistivity to the aging or loading conditions in comparison to the synthetically matrix be the reason for the significant different fracture behaviours? The results show the hypothetically relationship of crack initiation and propagation of rubber products based on nature or synthetic rubber. This phenomenon should be investigated according different fundamental rubbers (natural and synthetic) based on specific material structures and curing systems, whereas the localization of initiated cracks could pointed the structure of rubber matrix predisposed to lower resistivity to the fatigue failure. Besides the relationship of crack initiation and instable crack propagation at higher tearing energy should be investigated.

Crack surface

The crack surface exactly reflects the crack growth rate. The dissipative processes are governed in viscoelasticity due to dynamic loading, the material forces as crack driving forces hast to be applied and the relationship is focused to the vicinity of initiated crack tip[18]. The increase of tearing energy at high crack tip velocities in non-crystallising elastomers is due to viscoelastic dissipation in the vicinity of crack tip outside of the fracture process zone. This dissipation contribution can be ascribed to the decrease in the shear modulus in glass transition. Due to uncompressible behavior in the

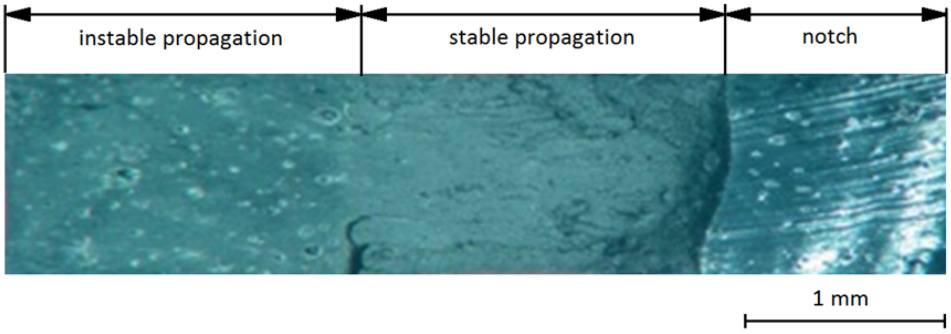

Fig. 6. **Fracture surface with denoting of the stable and instable are of crack propagation defined due to the different roughness. The crack propagation proceeds from the right to the left**

vicinity of the crack tip at low crack velocities respectively at low tearing energy, the volume of the material cannot increase as consequence of a positive hydrostatic stress unless cavity are formed. At high crack tip velocities respectively at high tearing energy, material dilatation is possible in the vicinity of the crack tip[19]. The fracture surfaces of rubber test specimens created by high velocity crack propagation are smooth on the macro-scale, whereas the fracture surfaces created by low crack tip velocity propagation are rather rough[19]. Therefore, the reason for instability in plot of the tearing energy against the crack tip velocity seems to be a transition in the fracture mechanism due to a change in volumetric behavior as a consequence of different deformation mechanisms of the material at short and long time. An exemplary fracture surface with the different roughness in the stable and instable crack propagation shows Fig. 6. This instability separates the stable and unstable crack propagation. In order to understand the processes within the fracture process zone the topography of fracture surface was by Horst et al.[20] investigated at various length scales. They described the fracture surface of filled rubber by different roughness exponents in different directions and denoted the surface as anisotropic. Horst et al.[18] founded the roughness exponents ζ = 0,87±0,03 along the crack front and ζ = 0,70±0,06 along the crack propagation direction within a certain range of length scale. Whereas Bouchaud et al.[21,22] founded the roughness exponents ζ = 0,80 for brittle materials. The crack surface observation in the all studies was performed on test specimen under the quasi-static loading conditions far from the initiated crack. There is no publication focused on observation and description of the crack surface formed under the dynamic loading conditions in the literature. Could the founded roughness exponents by Horst et al.[18] at quasi-static loading conditions correspond with the roughness of rubber crack surface created at dynamic loading conditions? What is the scale of roughness exponents for the instable crack growth at initiation of cracks?

Concept of future experimental analysis of micro-crack initiation

Firstly, the analysis will be fundamentally described. It is necessary to establish an experimental measurement, which firstly is able to localize the micro-cracks in the structure of rubber test specimen, initiated after the aging process. Secondarily it is necessary to create a new macro-crack due to fatigue crack growth analysis. The surface of created macro-cracks will contain exact localized micro-cracks. The microscopic description of the crack surface roughness exponent according to the crack growth rate in the location outside of micro-cracks in comparison to roughness exponent in location inside of micro-crack surface will exact evaluate the crack growth rate of micro-crack initiation. The microscopic observation of material structure of the micro-crack tip vicinity will explain the reason for the micro-crack initiation.

Secondarily we describe the analysis in more details. The initiation of instability is caused due to more main processes, which start with the micro-crack initiation. The aging at oxidative atmosphere is according to the first zone shown in the Fig. 4, the commonly proceeding process that influences the micro-crack initiation. The process of aging is linked to loss of mechanical properties over the whole life-time of the rubber product[23]. Huang et al.[24] studied the phenomenon of cyclic ageing on NR rubber. They found, that for NR rubber, aging at lower temperatures leads to a decrease in modulus, while at higher temperatures leads to an increase in modulus. Bauer et al.[25] studied the mechanical properties of skim tire based on BR rubber under the oxidative aging with fill gases 50/50 blend of N_2/O_2 at various temperatures in the range from 50 to 70 °C. They demonstrated the degreasing of elongation-to-break and increasing of modulus versus time of aging in the whole range of temperatures. This degrading in mechanical behaviour leads to high inclination of rubber material to the failure and proves the initiation of micro-cracks. Heinrich et al. in ref.[1] characterized the geometry of crack tip independent on the

crack length in relation to the thickness of the test specimen as linear line, which is oriented orthogonally to the main strain according to the fracture theory formulated by Rivlin and Thomas[10].

Thus for the experimental characterization of micro-crack initiation the pools of selected test specimens, according to the used following fatigue, fracture and impact analysis, shall to be aged in oxidative chamber of accelerated weathering testing instrument under the variation of temperature and pre-stress conditions.

X-ray computed tomography (CT) is the most important technique for a nondestructive visualizing interior features within solid objects, and for obtaining digital information on their 3D geometries. The using of tomography in the scale of micrometer allows to reconstruct the 3D geometry of test specimen and thus to localize the micro-crack position and geometry in the aged test specimens.

Generally the propagation of initiated micro-crack proceeds during strain at lower tearing energy and could firstly start with the high dynamic deformation of the object (for examples the contact of rolling tire with the profile of the road surface), which has considerable E-modulus in comparison with the deformed rubber part. After the proceeding of loading in the timing range of milliseconds the deformation is enable and strained rubber zone relaxes. This mechanism repeats in the frequency of real mechanical dynamic loading. The crack propagation corresponds with the applied process and is characterized due to the crack growth rate.

The dynamic crack growth behavior of vulcanized rubber is presently investigated in the SENT- as well as in pure-shear test specimens. The SENT test specimen is used in commercial studies of elasticity and fracture mechanics of rubber. But in classical studies of fracture mechanics of rubber the pure-shear test specimen featured prominently because of the amenability to a simple fracture mechanics analysis and large crack length used for characterization of its surface[10,15]. Stoček et al.[26] demonstrated that the values for tearing energies and also crack growth rates for short crack lengths in SENT- as well as in pure-shear test specimens are identical. On the other hand they observed different stable crack growth rate for short and large crack lengths at edge effect and in the pure-shear range, where the crack at large length propagates at higher rate. The definition of the pure-shear range in dependence of geometry ratio firstly was published in paper by Stoček et al.[26]. Thus a minimal allowed notch length in the test specimen, independent from its geometry, could be defined and the simple fracture mechanics analysis in pure-shear test specimens was possible effectively to use. The better qualitatively correlation with the orthogonally crack propagation to the main stress was evaluated in the pure-shear range of pure-shear test specimen in the comparison to the crack propagation in SENT test specimen[27]. Therefore the pure-shear test specimen and this method will also be recommended for determination of crack growth in rubber and characterization of crack surface. There is only one commonly used test equipment for the quantitatively description of dynamic crack growth working under the real dynamic loading conditions concerning to the independent loading function, based on SENT as well as pure-shear test specimens – Tear Analyzer manufactured by company Coesfeld GmbH[28].

According to the aim of the characterization of micro-crack initiation the fatigue crack growth analysis of test specimen pool under the real pulse-loading conditions is necessary to be analysed. The aged pure-shear test specimen shall to be used for the analysis. The crack growth rate and tearing energy over the complete analysis is necessary to observe.

Finally in order to understand precisely the influences of relationship between crack initiation and growth the structure of fracture surface, roughness profiles in the localized zone of initiated micro-crack and the surface far from this zone shall to be investigated by using of scanning electron microscopy (SEM), whereas the analysis is based on height-height correlation functions and observation of crack surface topology. The SEM derives from electron-sample interactions different information about the sample including external morphology as well as the chemical composition and for example crystalline structure. Thus the recognizing of structure component in rubber matrix, which is the reason for the micro-crack initiation can be performed. Areas ranging from approximately up to 1.5 nm could be imaged in a scanning mode using conventional SEM techniques.

Conclusion

The work is concerning with a description of possible experimental characterization of micro-crack's initiation and relationship to the crack growth in unfilled and filler reinforced elastomers under the real atmospheric and dynamic loading conditions supported by scaling and characterization of initiated and propagated crack surface. The determination of the crack surface roughness is the one of the most important factor, which characterize the crack growth velocity according to the fracture mechanical treatment of failure due to fatigue loading. The crack surface roughness can efficiently be performed according to the mathematical approach based on evaluation of roughness exponents in different crack propagation directions. The roughness exponents will characterize the derivation of relationships between different crack growth velocities at crack initiation and its propagation according to the different analysis, aging and loading conditions. Due to using of this simple experimental method, it will firstly be possible to characterize the reasons for micro-crack initiation as well as to define its crack growth velocity. Experimental works along these lines are in progress and will be reported on elsewhere.

This contribution was written with the support of the Operational Programme 'Education for Competitiveness' co-funded by the European Social Fund (ESF) and the national budget of the Czech Republic, project: Advanced Theoretical and Experimental Studies of Polymer Systems (reg. number: CZ.1.07/2.3.00/20.0104) and with the support of the Operational Programme 'Research and Development for Innovations' co-funded by the European Regional Development Fund (ERDF) and the national budget of the Czech Republic, project: Centre of Polymer Systems (reg. number: CZ.1.05/2.1.00/03.0111).

REFERENCES

1. Heinrich G., Klüppel M., Vilgis T. A.:. Curr. Opin. Solid State Mater. Sci. *6*, 195 (2002).
2. Klüppel M.: Adv. Polym. Sci. *164*, 1 (2003).
3. Dannenberg E. M.: Rubber Chem. Technol. *44*, 440 (1975).
4. Klüppel M., Schramm J.: An advanced micro-mechanical model of hyperelasticity and stress softening of reinforced rubbers. In: *Dorfmann, Muhr, editors, Constitutive models for rubber I*, Lisse: A.A. Balkema, pp. 211–220, 2000.
5. Raab A. L., Manas-Zloczower I., Feke D. L.: J. Colloid Interface Sci. *189*, 131 (1997).
6. Heinrich G., Klüppel M.: Adv. Polym. Sci. *160*, 1 (2002).
7. Vilgis T. A.: Polymer *46*, 4223 (2005).
8. Reincke K., Klüppel M., Grellmann W.: Kautsch. Gummi Kunstst. *62*, 246 (2009).
9. Klüppel M., Huang G., Bandow B.: Kautsch. Gummi Kunstst. *61*, 656 (2008).
10. Rivlin R. S., Thomas A. G.: J. Polym. Sci. *10*, 291 (1953).
11. Rice J. R., Rosengren G. F.: J. Mech. Phys. Solids *16*, 1 (1968).
12. Horst T., Heinrich G., Schneider M., Schulze A., Rennert M., in: *Fracture Mechanics & Statistical Mech.*, (W. Grellmann et al., ed.). LNACM 70, pp. 129–165, 2013.
13. Lake G. J.: Rubber Chem. Technol. *68*, 435 (1995).
14. Gent A. N., Lindley P. B., Thomas A. G.: J. Appl. Polym. Sci. *8*, 455 (1964).
15. Lake G. J., Lindley P. B.: J. Appl. Polym. Sci. *9*, 1233 (1965).
16. Paris P., Erdogan F.: J. Basic Eng., Transactions of the American Society of Mechanical Engineers, 528–534 (1963).
17. Person B. N. J., Albohr O., Heinrich. G., Ueba H.: J. Phys.: Condens. Matter *17*, R1071-R1142 (2005).
18. Horst T., Heinrich G.: Polym. Sci., Ser. A *50*, 5, 583 (2008).
19. Horst T.: *Spezifische Ansätze zur bruchmechanischen Charakterisierung von Elastomeren*, TUDpress, 2011.
20. Horst T., Reincke K., Ilisch S., Heinrich G., Grellmann W.: Phys. Rev. E *80*, 046120 (2009).
21. Bouchaud E.: Surf. Rev. Lett. *10*, 797 (2003).
22. Bouchaud E., Lapasset G., Planes J.: Europhys. Lett. *13*, 73 (1990).
23. Baldwin J. M., Bauer D. R., Ellwood K. R.: Polym. Degrad. Stab. *92*, 103 (2007).
24. Huang D., LaCount B. J., Castro J. M., Ignatz-Hoover F.: Polym. Degrad. Stab. *74*, 353 (2001).
25. Bauer D. R., Baldwin J. M., Ellwood K. R.: Polym. Degrad. Stab. *92*, 110 (2007).
26. Stoček R., Heinrich G., Gehde M., Rauschenbach A.: Int. J. Plast. Technol. 2–22 (2012).
27. Stoček R., Heinrich G., Gehde M., Kipscholl R.: Kautsch. Gummi Kunstst. *65*, 49 (2012).
28. Eisele U., Kelbch S. A., Engels H.-W.: Kautsch. Gummi Kunstst. *45*, 1064 (1992).